

Immature MEF2C-dysregulated T-cell leukemia patients have an early T-cell precursor acute lymphoblastic leukemia gene signature and typically have non-rearranged T-cell receptors

Linda Zuurbier,¹ Alejandro Gutierrez,^{2,3} Charles G. Mullighan,⁴ Kirsten Canté-Barrett,¹ A. Olivier Gevaert,⁵ Johan de Rooi,^{6,7} Yunlei Li,¹ Willem K. Smits,¹ Jessica G.C.A.M. Buijs-Gladdines,¹ Edwin Sonneveld,⁸ A. Thomas Look,^{2,3} Martin Horstmann,^{9,10} Rob Pieters,^{1,8} and Jules P.P. Meijerink¹

¹Department of Pediatric Oncology/Hematology, Erasmus MC Rotterdam-Sophia Children's Hospital, Rotterdam, the Netherlands; ²Department of Pediatric Oncology, Dana-Farber Cancer Institute, Boston, MA, USA; ³Division of Hematology/Oncology, Children's Hospital, Boston, MA, USA; ⁴Department of Pathology, St Jude Children's Research Hospital, Memphis, TN, USA; ⁵Center for Cancer Systems Biology (CCSB) and Department of Radiology, Stanford University School of Medicine, Stanford, CA, USA; ⁶Department of Biostatistics, Erasmus MC Rotterdam, Rotterdam, the Netherlands; ⁷Department of Bioinformatics, Erasmus MC Rotterdam, Rotterdam, the Netherlands; ⁸Dutch Childhood Oncology Group (DCOG), the Hague, the Netherlands; ⁹German Cooperative Study Group for Childhood Acute Lymphoblastic Leukemia (COALL), Hamburg, Germany; and ¹⁰Research Institute Children's Cancer Center Hamburg, Clinic of Pediatric Hematology and Oncology, University Medical Center Hamburg-Eppendorf, Hamburg, Germany

©2013 Ferrata Storti Foundation. This is an open-access paper. doi:10.3324/haematol.2013.090233

Manuscript received on April 22, 2013. Manuscript accepted on August 20, 2013.

Correspondence: j.meijerink@erasmusmc.nl

Online methods

Immature *MEF2C*-dysregulated T-cell leukemia patients have an early T-cell precursor acute lymphoblastic leukemia gene signature and typically have non-rearranged T-cell receptors

Linda Zuurbier¹, Alejandro Gutierrez^{2,3}, Charles G. Mulighan⁴, Kirsten Canté-Barrett¹, A. Olivier Gevaert⁵, Johan de Rooi^{6,7}, Yunlei Li¹, Willem K. Smits¹, Jessica G.C.A.M. Buijs-Gladdines¹, Edwin Sonneveld⁸, A. Thomas Look^{2,3}, Martin Horstmann^{9,10}, Rob Pieters^{1,8}, and Jules P.P. Meijerink¹

¹Department of Pediatric Oncology/Hematology, Erasmus MC Rotterdam-Sophia Children's Hospital, Rotterdam, the Netherlands;

²Department of Pediatric Oncology, Dana-Farber Cancer Institute, Boston, MA, USA;

³Division of Hematology/Oncology, Children's Hospital, Boston, MA, USA;

⁴Department of Pathology, St Jude Children's Research Hospital, Memphis, TN, USA;

⁵Center for Cancer Systems Biology (CCSB) & Department of Radiology, Stanford University School of Medicine, Stanford, CA, USA;

⁶Department of Biostatistics, Erasmus MC Rotterdam, Rotterdam, the Netherlands;

⁷Department of Bioinformatics, Erasmus MC Rotterdam, Rotterdam, the Netherlands;

⁸Dutch Childhood Oncology Group (DCOG), the Hague, the Netherlands;

⁹German Cooperative Study Group for Childhood Acute Lymphoblastic Leukemia (COALL), Hamburg, Germany;

¹⁰Research Institute Children's Cancer Center Hamburg, Clinic of Pediatric Hematology and Oncology, University Medical Center Hamburg-Eppendorf, Hamburg, Germany

Fluorescent in-situ hybridization (FISH). FISH analysis was performed on thawed cytospin slide as described before.(1) To identify rearrangements of the *LYL1* locus, we used home-labeled BAC clones RP11-352L7 and RP11-356L15 (BAC/PAC Resource Center, Children's Hospital, Oakland, USA).

Genomic DNA and RNA extraction and ABD status detection by quantitative PCR

Genomic DNA and RNA were isolated from $\geq 5 \times 10^6$ leukemic cells using TRIzol reagent (Invitrogen) according to the manufacturer's protocol, with minor modifications.(2) DNA was stored at 4°C. For RNA isolation, an additional phenol-chloroform extraction was performed as a minor modification of the protocol, and RNA was precipitated with isopropanol together with 1 μ l (20 μ g/ml) glycogen (Roche, Almere, the Netherlands). After precipitation, the RNA pellets were dissolved in 20 μ l RNase-free TE buffer (10 mM Tris-HCl, 1 mM EDTA, pH 8.0), and the concentration was measured spectrophotometrically.(2) The presence of absence of bi-allelic *TRG* deletions (ABD) was determined using quantitative PCR, targeting the intron between TRGV11 and TRGJP1 as described previously.(3)

***In vitro* cytotoxicity assay**

In vitro cytotoxicities for leukemic cells towards serial dilutions of L-Asparaginase (0.003-10 IU/mL, Paronal, Christiaens, Breda, The Netherlands), prednisolone (0.08-250 µg/mL, BUFA BV, Uitgeest, the Netherlands), vincristine (0.05-50 µg/mL TEVA Pharma BV, Mijdrecht, The Netherlands), daunorubicin hydrochloride (0.002-2.0 µg/mL, Ceubidine, Rhône-Poulenc Rorer, Amstelveen, The Netherlands) or cytarabine (0.002-2.5 µg/mL, Cytosar, Pharmacia & Upjohn, Woerden, the Netherlands) were determined using the MTT assay.(4) Briefly, 1.6×10^5 leukemic cells (>90% purity as determined by morphological examination of May-Grunwald-Giemsa (Merck, Darmstadt, Germany) stained cytopsin slides) were exposed to serial dilutions of chemotherapeutic drugs in duplicate in a final volume of 100 µL culture media (RPMI 1640 (Life Technologies, Breda, The Netherlands) supplemented with 10% fetal calfs serum (Integro, Zaandam, The Netherlands), 5 µg/mL transferrin, 5 ng/mL sodium selenite (ITS media supplement, Sigma-Aldrich, Zwijndrecht, The Netherlands), 100 IU/mL penicillin, 100 µg/mL streptomycin, 0.125 µg/mL fungizone (Life technologies)). Following 4 days of incubation in a humified incubator at 37°C with 5% CO₂, 5 mg/mL MTT (3-[4,5-dimethyl-diazol-2-yl]-2,5-diphenyl-tetrazolium-bromide, Sigma-Aldrich) was added and incubated for an additional 6 hrs at 37°C to facilitate reduction of MTT tetrazolium salt into formazan crystals by viable cells. Total formazan production was measured spectrophotometrically at 562 nm. For each patient sample, leukemic cells incubated in the absence of drugs was used as control, whereas the assay performed on pure media containing wells were used for background correction (blank values). Leukemic cells survival following exposure to each drug concentration was calculated for background corrected OD values using the formula: $((OD \text{ drug incubated wells} / OD \text{ control wells}) \times 100\%)$, and the LC50 drug concentrations, at which 50% of the leukemic cells die, were calculated.

Microarray expression analyses

RNA integrity testing, copy-DNA and copy-copy RNA (ccRNA) syntheses, washing, hybridization to Human Genome U133 plus 2.0 microarrays (Affymetrix, Santa Clara, CA), extraction of probe set intensities from CEL-files and normalization with RMA or VSN methods were performed as previously described.(1)

Geneset enrichment analysis (GSEA; (5)) was performed on our Affymetrix U133 plus 2.0 microarray expression dataset for 117 T-ALL cases(6) using 1000 random permutations . Enrichment scores and nominal p-values were obtained for up- or down-regulated probe sets among the TOP100, 200 or 500 most significantly, differentially expressed probesets for human ETP-ALL compared to other T-ALL cases.(7) Also up- or down-regulated genes or

probesets for C/EBPA-mutated AML(8) and early T-cell (MPP-ETP-DN2A) and committed T-cell (DN2B-and later) subsets(9) were tested.

ETP-ALL patients were identified by Prediction Analysis of Microarrays (PAM) (10) implemented in *R* (11) using the human ETP-ALL probe set signature.(7) The classifier was built on the 100, 200 or 500 most significant probe sets from this ETP-ALL gene signature (**Supplementary Table S1**) (7) using class labels immature cluster (n=15) and non-immature cluster (n=102) in our gene expression cohort comprising 117 T-ALL patient samples. Patients with a cross-validated probability greater than 0.6 for being classified as immature were considered to be ETP-ALL patients. Microarray data are available at the gene expression omnibus (<http://www.ncbi.nlm.nih.gov/geo/>), accession GSE10609 and GSE26713.

Differentially expressed genes between ETP-ALL cases with or without bi-allelic *TRG@* rearrangements (ABD versus non-ABD ETP-ALL) were obtained by regression analysis using the *limma* package in the R statistical software package.(11) VSN- or RMA-normalized expression values for *MEF2C* (probe set 239966_at), *LMO1* (probe set 206718_at), *LMO2* (probe set 204249_s_at), *LYL1* (probe set 210044_s_at), *ERG1* (probeset 1563392_at) and *BAALC* (probe set 222780_s_at) were used to test for differential expression between the T-ALL groups (representative probe sets were used).

Human hematopoietic progenitor signature genes (probesets) as established by Novershtern and coworkers(12) within the immature cluster gene signature were enriched using the Fisher's exact test. Differentially expressed genes between the immature cluster (n=15) (13) versus other T-ALL cases (n=102) in our T-ALL microarray expression set were analyzed using the Wilcoxon statistical test and corrected for multiple testing error using the false discovery rate procedure as previously described(14) using the Bioconductor package Multitest. A total of 784 probesets with an FDR p-value less than p=0.01 was selected as the immature cluster expression signature gene set (**Supplementary Table S5**).

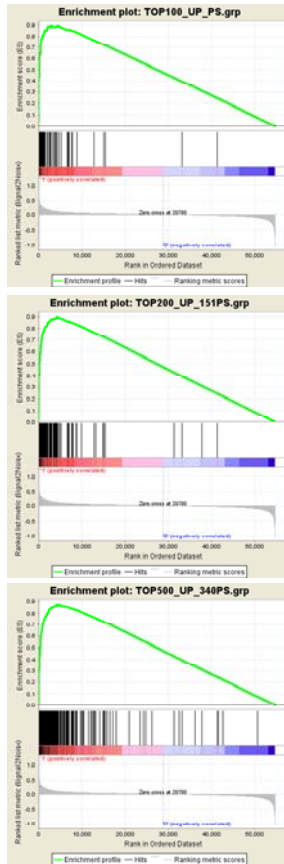
References

1. Van Vlierberghe P, Pieters R, Beverloo HB, Meijerink JP. Molecular-genetic insights in paediatric T-cell acute lymphoblastic leukaemia. *Br J Haematol*. 2008 Oct;143(2):153-68.
2. Stam RW, den Boer ML, Meijerink JP, Ebus ME, Peters GJ, Noordhuis P, et al. Differential mRNA expression of Ara-C-metabolizing enzymes explains Ara-C sensitivity in MLL gene-rearranged infant acute lymphoblastic leukemia. *Blood*. 2003 Feb 15;101(4):1270-6.
3. Gutierrez A, Dahlberg SE, Neuberg DS, Zhang J, Grebliunaite R, Sanda T, et al. Absence of Biallelic TCR{gamma} Deletion Predicts Early Treatment Failure in Pediatric T-Cell Acute Lymphoblastic Leukemia. *J Clin Oncol*. 2010 Aug 20;28(24):3816-23.
4. Den Boer ML, Harms DO, Pieters R, Kazemier KM, Gobel U, Korholz D, et al. Patient stratification based on prednisolone-vincristine-asparaginase resistance profiles in children with acute lymphoblastic leukemia. *J Clin Oncol*. 2003 Sep 1;21(17):3262-8.

5. Subramanian A, Tamayo P, Mootha VK, Mukherjee S, Ebert BL, Gillette MA, et al. Gene set enrichment analysis: a knowledge-based approach for interpreting genome-wide expression profiles. *Proc Natl Acad Sci U S A*. 2005 Oct 25;102(43):15545-50.
6. Homminga I, Pieters R, Langerak A, de Rooi JJ, Stubbs A, Buijs-Gladdines J, et al. Integrated transcript and genome analyses reveal NKX2-1 and MEF2C as potential oncogenes in T -cell acute lymphoblastic leukemia. *Cancer Cell*. 2011:April 11th. [Epub ahead of print].
7. Zhang J, Ding L, Holmfeldt L, Wu G, Heatley SL, Payne-Turner D, et al. The genetic basis of early T-cell precursor acute lymphoblastic leukaemia. *Nature*. 2012 Jan 12;481(7380):157-63.
8. Wouters BJ, Jorda MA, Keeshan K, Louwers I, Eipelink-Verschuere CA, Tieleman D, et al. Distinct gene expression profiles of acute myeloid/T-lymphoid leukemia with silenced CEBPA and mutations in NOTCH1. *Blood*. 2007 Nov 15;110(10):3706-14.
9. Mingueneau M, Kreslavsky T, Gray D, Heng T, Cruse R, Ericson J, et al. The transcriptional landscape of alphabeta T cell differentiation. *Nat Immunol*. 2013 Jun;14(6):619-32.
10. Tibshirani R, Hastie T, Narasimhan B, Chu G. Diagnosis of multiple cancer types by shrunken centroids of gene expression. *Proc Natl Acad Sci U S A*. 2002 May 14;99(10):6567-72.
11. Team RDC. R: A Language and Environment for Statistical Computing. 2011.
12. Novershtern N, Subramanian A, Lawton LN, Mak RH, Haining WN, McConkey ME, et al. Densely interconnected transcriptional circuits control cell states in human hematopoiesis. *Cell*. 2011 Jan 21;144(2):296-309.
13. Homminga I, Pieters R, Langerak AW, de Rooi JJ, Stubbs A, Verstegen M, et al. Integrated transcript and genome analyses reveal NKX2-1 and MEF2C as potential oncogenes in T cell acute lymphoblastic leukemia. *Cancer Cell*. 2011 Apr 12;19(4):484-97.
14. Hochberg Y, Benjamini Y. More powerful procedures for multiple significance testing. *Stat Med*. 1990 Jul;9(7):811-8.

Supplementary Figure S1.

A

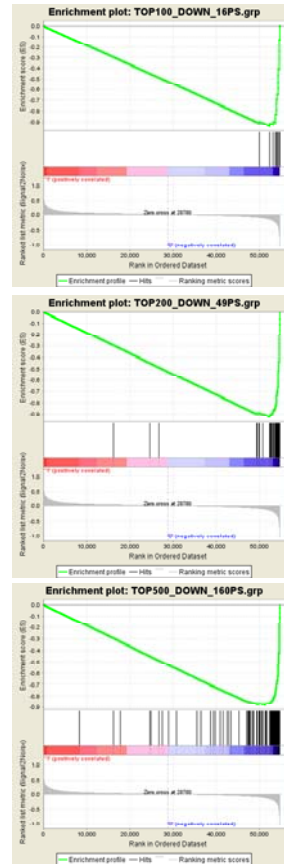


1000 permutations
Upregulated in Immature
84 probesets
ES= 0.8906417
NES= 1.7610614
NOM P-value<0.0001
FDR<0.0001

1000 permutations
Upregulated in Immature
151 probesets
ES= 0.8929122
NES= 1.8345773
NOM P-value<0.0001
FDR<0.0001

1000 permutations
Upregulated in Immature
340 probesets
ES= 0.8715323
NES= 1.9051393
NOM P-value<0.0001
FDR<0.0001

B

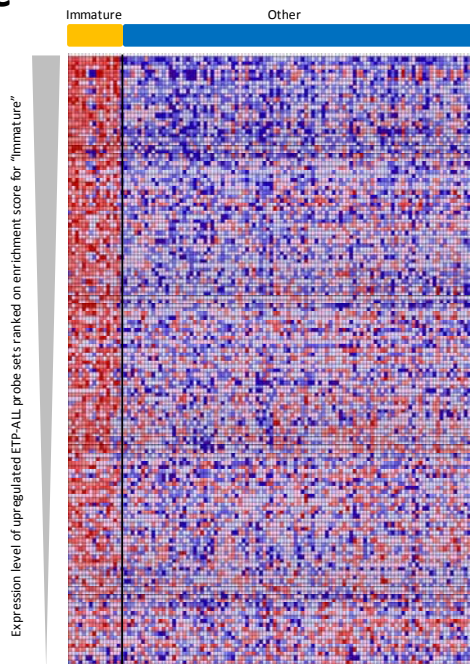


1000 permutations
Down regulated in Immature
16 probesets
ES= -0.9412975
NES= -1.5765783
NOM P-value<0.0001
FDR<0.0001

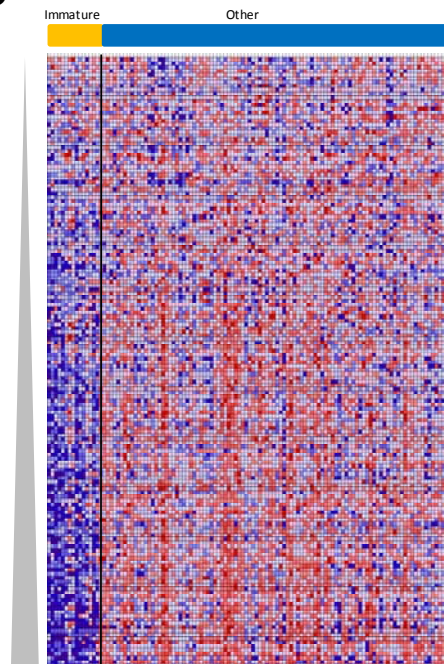
1000 permutations
Down regulated in Immature
49 probesets
ES= -0.9274382
NES= -1.688663
NOM P-value<0.0001
FDR<0.0001

1000 permutations
Down regulated in Immature
160 probesets
ES= -0.8799995
NES= -1.7953509
NOM P-value<0.0001
FDR<0.0001

C

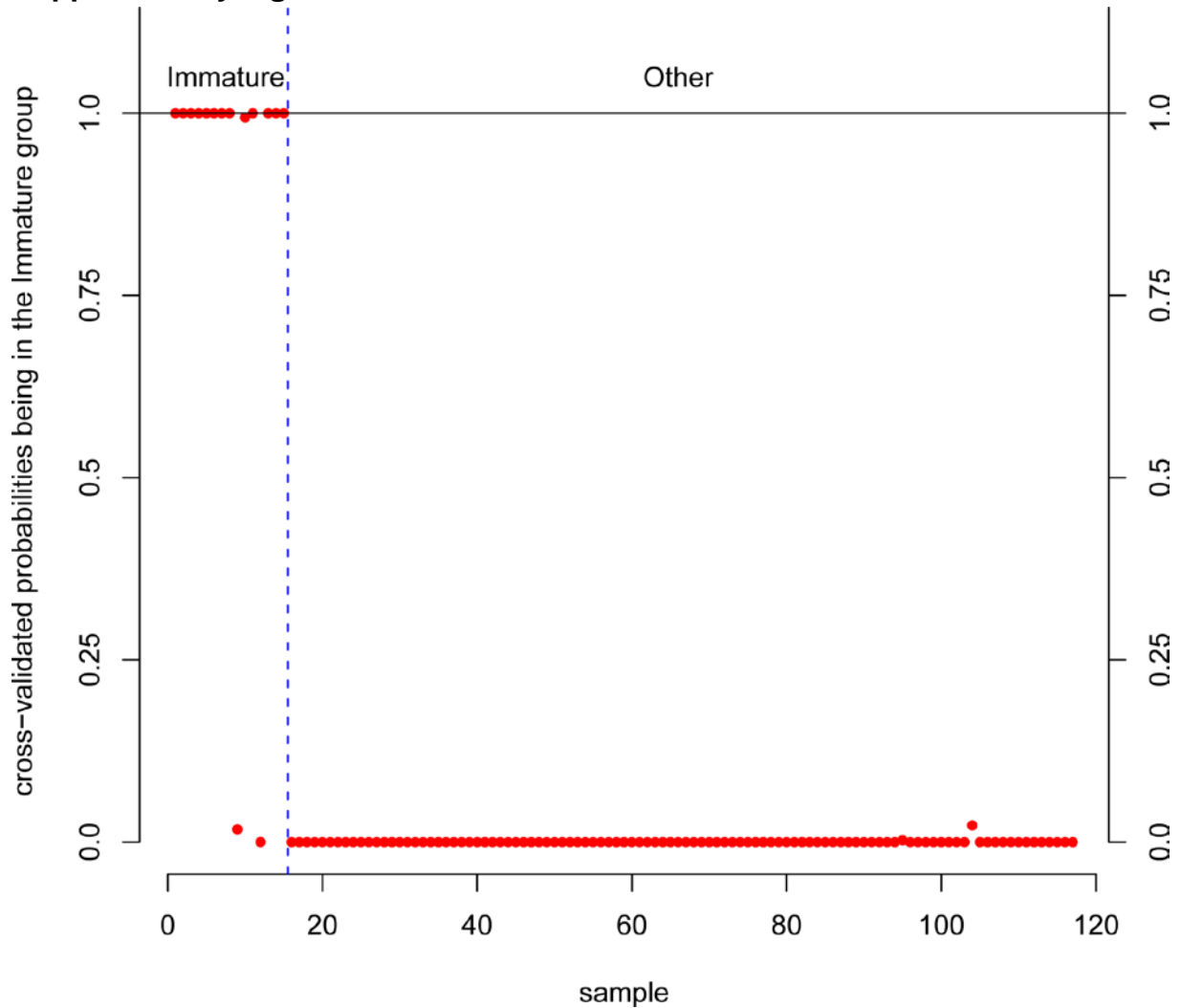


D



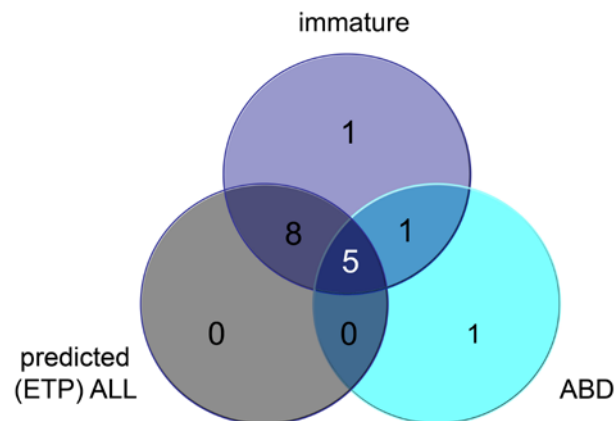
ETP-ALL signatures genes are enriched in the immature T-ALL cluster. Gene set enrichment analysis (GSEA) for **(A)** up- and **(B)** down-regulated probe sets from the top 100, 200 or 500 most significantly differentially expressed probe sets from the human ETP-ALL gene signature (Zhang *et al.*, nature 2012) for immature cluster versus other T-ALL patients. Significance levels for each analysis have been indicated. Heatmaps for **(C)** up- and **(D)** down-regulated probe sets for immature cluster patients versus other T-ALL patients.

Supplementary Figure S2.



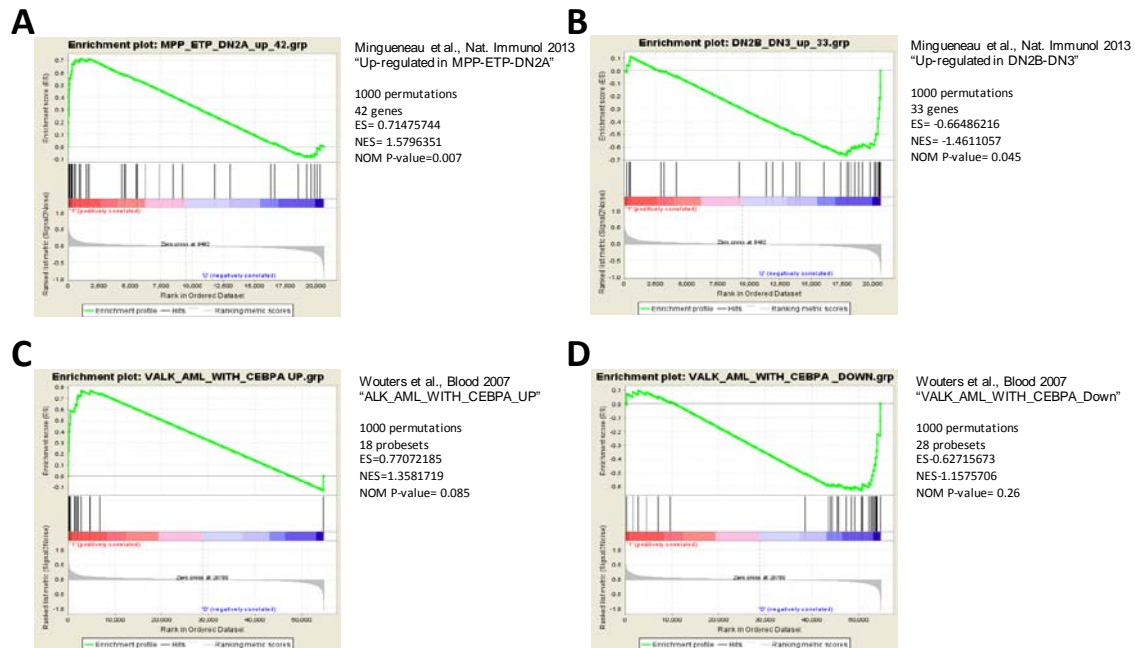
PAM prediction of immature cluster cases versus non-immature cluster T-ALL patients based on the TOP100, 200 or 500 most significant probe sets from the human ETP-ALL gene signature (Zhang *et al.*, Nature 2012). Only results for the TOP100 most significant ETP-ALL gene signature probe sets are shown predicting 13 out of 15 immature cluster cases while none of the 102 non-immature cluster cases on this probe selection ($p < 0.001$).

Supplementary Figure S3.



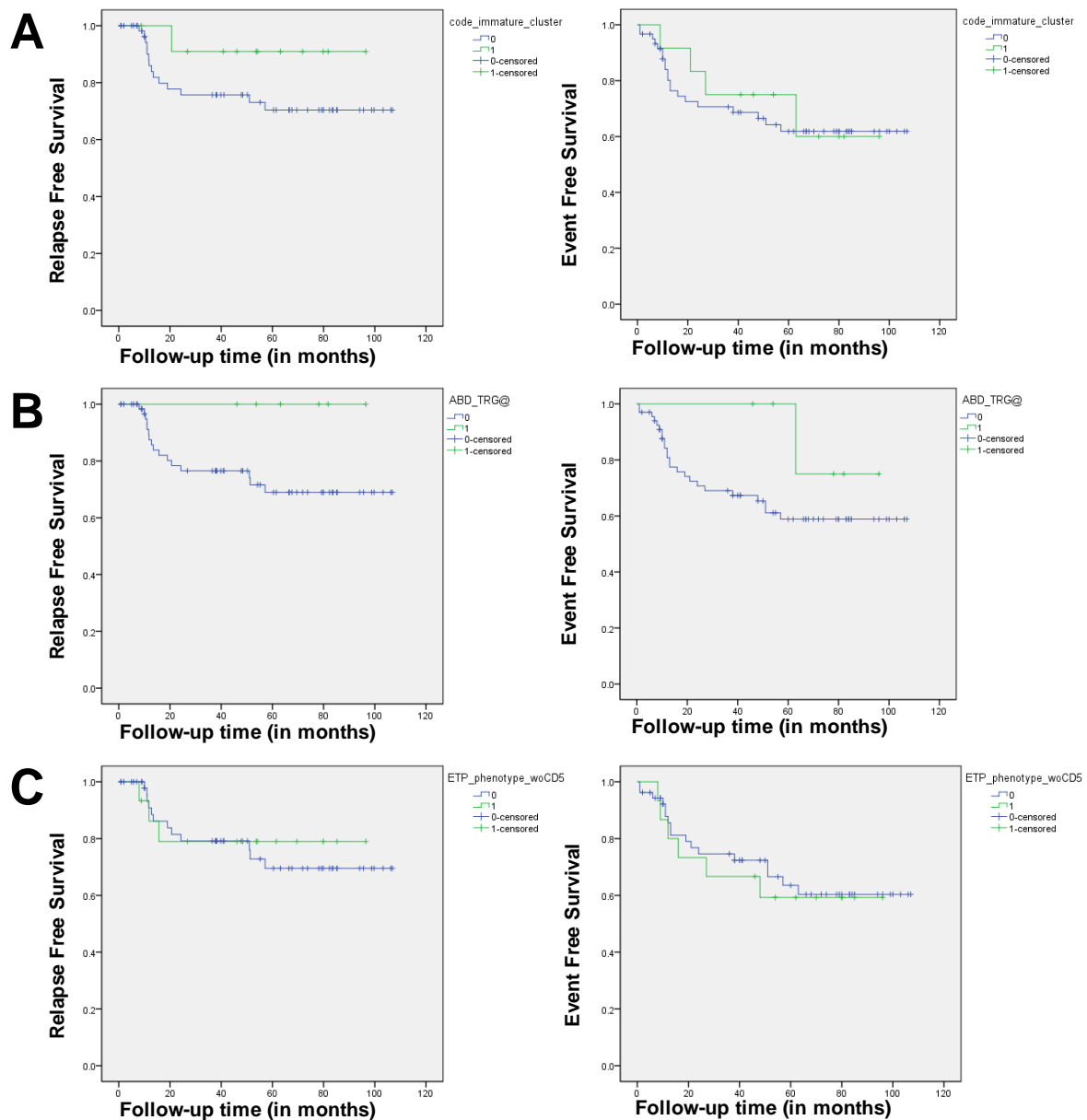
Overlap between the immature cluster, ETP-ALL and ABD characteristics in our pediatric T-ALL cohort. The number of ETP-ALL positive patients in this Venn diagram is depicted by the gray sphere, the number of ABD patients is depicted by blue sphere, and the number of immature cluster patients is depicted by the dark blue sphere. This diagram is based on 117 T-ALL patients for whom gene expression array data is available.

Supplementary Figure S4.



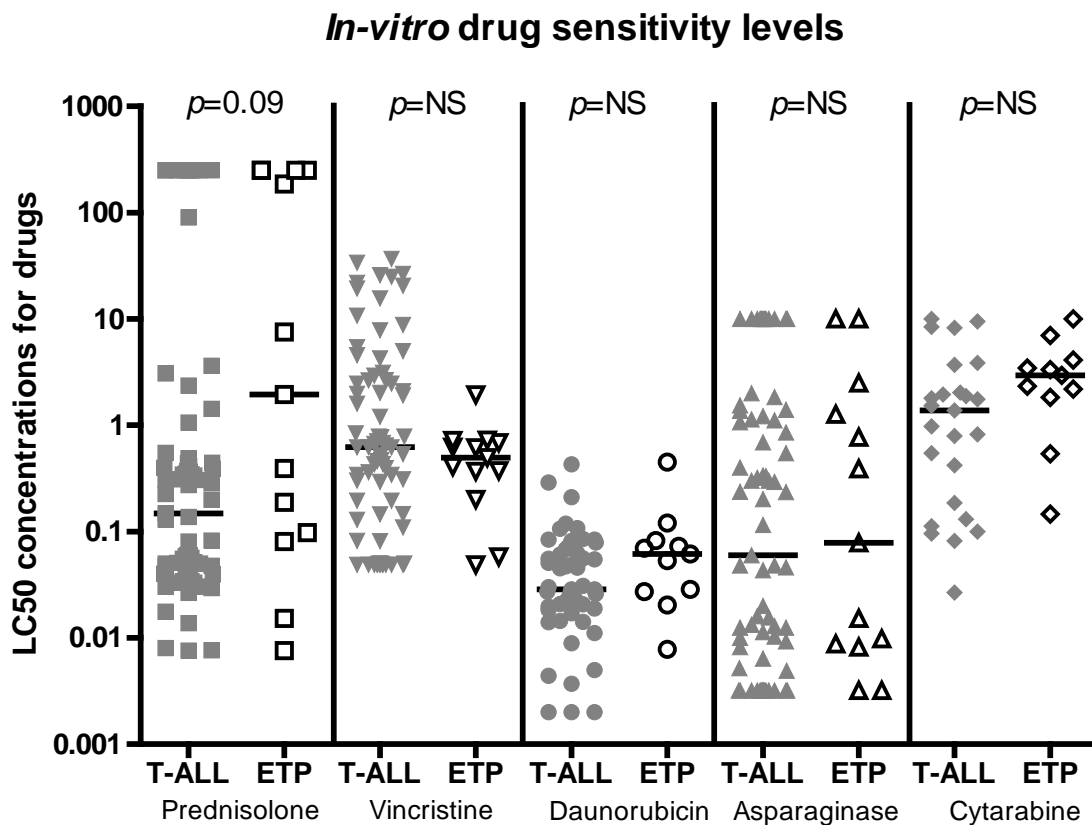
Immature cluster/ETP-ALL cases are enriched for early T-cell development signatures. Enrichment of **(A)** MPP-ETP-DN2A or **(B)** post-DN2A T-cell signature genes in immature cluster/ETP-ALL T-ALL cases. GSEA for **(C)** up- or **(D)** down-regulated genes of *C/EBPA*-inactivated AML patient samples in immature cluster/ETP-ALL T-ALL cases.

Supplementary Figure S5.



Immature cluster T-ALL, ABD and immunophenotypic ETP-ALL patients treated on the COALL-97 protocol do not predict for poor outcome. Relapse free survival (RFS) and event free survival (EFS) curves for COALL-97 pediatric T-ALL patients. RFS and EFS curves (**A**) for immature cluster T-ALL cases upon unsupervised cluster (green line) versus other T-ALL cases (blue line), (**B**) for ABD T-ALL cases (green line) versus non-ABD cases (blue line), and (**C**) for ETP-ALL cases as identified upon immunophenotypic parameters (green line) compared to other T-ALL cases (blue line). Cases that are lost from further follow-up are represented by vertical tick marks.

Supplementary Figure S6.



***In vitro* sensitivity of Immature cluster/ETP-ALL leukemic cells towards chemotherapeutic agents.** *In vitro* drug sensitivity levels towards prednisolone (squares), vincristine (downside-facing triangles), daunorubicin (circles), L-asparaginase (upside-facing triangles) and cytarabine (diamonds) were measured for leukemic cells of Immature cluster/ETP-ALL patients (open symbols) versus other T-ALL cases (closed gray symbols). The sensitivity level for each sample is indicated as the LC50 drug concentration that is lethal for 50 percent of the leukemic cells. Significance levels have been indicated. NS, not significant.

482	1556461_PM_at	---	---	0.91882865	0.977220596	4.125772538	4.077948316	0.047824	1.03370478
483	240765_PM_at	---	---	0.028595949	0.227118464	6.642139437	6.455397762	0.186742	1.13819021
484	228768_PM_at	FNIP1	NM_001008738 / NM	0.07222766	0.360051723	7.28922146	7.256492113	0.032729	1.02294554
485	218999_PM_at	TMEM140	NM_018295	0.030421855	0.234467851	6.58696476	6.397855417	0.189109	1.14005968
486	225551_PM_at	C1orf71	NM_001139459 / NM	0.79103701	0.935781481	5.330143948	5.348603262	-0.01846	-1.01287723
487	213241_PM_at	PLXNC1	NM_005761	2.04601E-05	0.003160045	5.795718173	4.917876847	0.877841	1.83762365
488	205505_PM_at	GCNT1	NM_001097633 / NM	0.639224834	0.871431152	6.913242985	7.112163205	-0.19892	-1.14783894
489	241816_PM_at	C14orf106	NM_018353	0.005642617	0.090578417	7.498696802	6.950447788	0.548249	1.46230983
490	210980_PM_s_at	ASAH1	NM_001127505 / NM	0.047122935	0.291783289	5.312206999	4.940204737	0.372002	1.29414768
491	219456_PM_s_at	RIN3	NM_024832	0.032347027	0.241245898	6.748192491	6.280217674	0.467975	1.38316649
492	206683_PM_at	ZNF165	NM_003447	8.95112E-05	0.007494682	4.707346103	3.927484665	0.779861	1.71696596
493	232500_PM_at	C20orf74	NM_020343	0.000105913	0.008296261	5.518459793	4.907859957	0.6106	1.52689392
494	1560762_PM_at	LOC285972	---	0.008976182	0.119208112	3.938687315	3.821208209	0.117479	1.08483761
495	204859_PM_s_at	APAF1	NM_0011160 / NM_01	0.922064651	0.978945328	4.579414874	4.568712555	0.010702	1.00744587
496	39650_PM_s_at	PCNXL2	NM_014801	5.07968E-06	0.001322584	6.293850992	6.903830552	-0.60998	-1.52623758
497	204849_PM_at	TCFL5	NM_006602	9.03064E-06	0.001870266	6.137567593	7.754904058	-1.61734	-3.06808077
498	229872_PM_s_at	LOC100132	XM_001722799	0.012750469	0.144483291	7.454216424	9.365594943	-1.91138	-3.76168363
499	231395_PM_at	ATP8A2	NM_016529	0.001974994	0.048927416	5.591332664	5.780016425	-0.18868	-1.13972342
500	218900_PM_at	CNNM4	NM_020184	0.002808215	0.060330841	6.667732625	6.353086006	0.314647	1.24370698

Supplementary Table S2. Immunophenotype of the immature cluster, ETP-ALL, and ABD T-ALL patients and patients with an ETP immunophenotype

Patient	unsupervised cluster <i>n</i> =15/117	ETP-ALL	ETP-ALL	ETP-ALL	ETP-ALL	ABD status <i>n</i> =7/117	simplified ETP-ALL immunophenotype		CD8 % positive	CD4 % positive	CD1 % positive	CD5 % positive	CD34 % positive	CD13 % positive	CD33 % positive
		probability PAM top100 <i>n</i> =13/117	probability PAM top200 <i>n</i> =13/117	probability PAM top500 <i>n</i> =13/117	summary PAM		including CD5 (≤75%)	excluding CD5 criteria							
9194	immature	1	1	1	ETP-ALL	one copy retained	yes	yes	1	1	1	7	2	NA	40
572	immature	1	1	1	ETP-ALL	both copies retained	-	yes	2	3	0	96	59	0	0
1524	immature	1	1	1	ETP-ALL	both copies retained	-	yes	3	1	2	97	53	3	66
1964	immature	1	1	1	ETP-ALL	both copies retained	-	yes	3	3	0	92	72	66	86
10030	immature	1	1	1	ETP-ALL	both copies retained	NA	NA	1	1	NA	56	1	0	0
167	immature	1	1	1	ETP-ALL	deleted	-	yes	16	2	14	90	45	0	0
321	immature	1	1	1	ETP-ALL	deleted	-	yes	6	5	6	97	35	2	60
491	immature	1	1	1	ETP-ALL	deleted	-	-	3	1	23	95	22	2	15
2130	immature	1	1	1	ETP-ALL	deleted	-	yes	21	0	0	88	67	0	5
9577	immature	1	1	1	ETP-ALL	deleted	-	-	15	9	66	80	0	0	4
2736	immature	1	1	1	ETP-ALL	deleted	yes	yes	1	1	0	2	69	2	44
1509	immature	1	1	1	ETP-ALL	deleted	yes	yes	4	3	0	7	6	NA	39
2703	immature	0.99	1	1	ETP-ALL	deleted	-	yes	1	0	8	92	79	3	0
2252	immature	0.02	0	0	-	deleted	-	-	93	73	90	95	7	2	2
9105	immature	0	0	0	-	one copy retained	-	-	83	68	7	83	0	0	0
9012	TLX	0	0.36	1	-	deleted	-	-	3	13	10	96	ND	ND	ND
9226	TAL/LMO	0	0	0	-	deleted	-	-	3	2	6	96	2	10	10
8639	TLX	0	0	0	-	deleted	-	-	0	96	3	95	0	0	0
9421	TLX	0.02	0.06	0.28	-	deleted	yes	yes	17	10	7	65	82	0	40
231	TAL/LMO	0	0	0	-	one copy retained	-	-	83	43	60	80	95	3	5
2750	TLX	0	0	0	-	deleted	-	yes	1	69	0	94	0	0	28
10111	TAL/LMO	0	0	0	-	deleted	-	yes	3	2	1	95	79	1	4
9858	TLX	0	0	0	-	deleted	-	yes	4	68	2	97	67	NA	4
720	TLX	0	0	0	-	deleted	-	yes	0	83	11	96	39	0	0
2780	TLX	0	0	0	-	deleted	yes	yes	7	57	6	70	7	28	28
1753	TAL/LMO	0	0	0	-	deleted	-	yes	6	6	4	90	49	0	0
585	TLX	0	0	0	-	deleted	-	yes	17	17	17	86	86	16	20
1032	TAL/LMO	0	0	0	-	deleted	-	yes	7	10	0	95	88	0	0
1632	TAL/LMO	0	0	0	-	deleted	-	yes	9	31	22	94	53	15	5
9963	TAL/LMO	0	0	0	-	deleted	-	yes	3	1	15	93	83	14	0

The immature, ETP-ALL and ABD patients are depicted in bold. ETP-ALL, early T-cell precursor ALL; ABD, absence of bi-allelic deletions; Unsupervised subgroups have been published (Homminga *et al.*, Cancer Cell 2011). The ETP-ALL immunophenotype for the DCOG and COALL cohorts was based on <25% expression of CD1 and CD8≥25% expression of CD13, CD33 or CD34 with or without ≤75% expression, and are shown in bold.

Supplementary Table S3. Overall clinical, immunophenotypic and molecular cytogenetic characteristics of the immature cluster (MEF2C) versus non-immature cluster T-ALL patients

	Immature Cluster				p-value	Bonferroni-Holm alpha
	-		+			
	n	(%) or range	n	(%) or range		
Total	102	(89%)	15	(11%)		
Clinical (n=117)						
Gender						-
Male	75		8		0.13	
Female	27		7			
Median age yrs (range)	7.8	(1.5-17.8)	10.1	(3.1-16.4)	0.51*	-
Median WBC x10e9 cells/liter (range)	120	(2-900)	88	(2-435)	0.062*	-
ETP-immunophenotype: CD5 (≤75%) (n=111)						
ETP immunophenotype	2	(2%)	3	(20%)	0.017	0.0033
non ETP immunophenotype	94	(98%)	12	(80%)		
CD1-, CD4/CD8 DN, CD34/CD33/CD13+ (n=111)						
yes	6	(6%)	10	(67%)	<0.001	0.0029
no	90	(94%)	5	(33%)		
Chromosomal rearrangements (n=117)						
TAL1/2/LYL1 (n=27)	27	(26%)	0	(0%)	0.021	0.0036
LMO1/2/3 (n=14)	14	(14%)	0	(0%)	0.21	
TLX3 (n=22)	22	(22%)	0	(0%)	0.07	
TLX1 (n=7)	7	(7%)	0	(0%)	0.59	
HOXA (n=10)	7	(7%)	3	(20%)	0.12	
MEF2C (n=6)	0	(0%)	6	(40%)	<0.001	0.0029
NKX2-1/NKX2-2 (n=7)	7	(7%)	0	(0%)	0.59	
Unknown (n=26)	20	(19%)	6	(40%)	0.097	
NOTCH1/FBXW7 status (n=112)						
wild-type (n=42)	36	(37%)	6	(40%)	1#	
mutant (n=70)	61	(63%)	9	(60%)		
PTEN/AKT status (n=113)						
wild-type (n=92)	79	(81%)	13	(87%)	0.73	
mutant (n=21)	19	(19%)	2	(13%)		
PHF6 status (n=41)						
wild-type (n=32)	29	(76%)	3	(100%)	1	
mutant (n=9)	9	(24%)	0	(0%)		
WT1 status (n=115)						
wild-type (n=101)	86	(86%)	15	(100%)	0.21	
mutant (n=14)	14	(14%)	0	(0%)		

Unsupervised clusters are explained in the legend for Table 3. Significant *p*-values are indicated in bold. The *p*-values were calculated using the Fisher's exact test or the Pearson's Chi-square test (#) instead: *Mann-Whitney *U* test; ^The significance level of immature cluster frequencies for the indicated cytogenetic subtype was compared to all other subtypes. WBC, white blood cell count. Bonferroni-Holm significance level for multiple testing correction is indicated.

Supplementary Table S4. Overall clinical, immunophenotypic and molecular cytogenetic characteristics of ABD versus non-ABD T-ALL patients

	ABD				p-value	Bonferroni-Holm alpha
	-		+			
	n	(%) or range	n	(%) or range		
Total	110	(89%)	7	(11%)		
Clinical (n=117)						
Gender						
Male	81		3		0.1	-
Female	29		4			
Median age yrs (range)	7.7	(1.5-17.8)	10.8	(5.4-16.1)	0.13*	-
Median WBC x10e9 cells/liter (range)	120	(2-900)	15	(2-248)	0.002*	0.003
ETP-immunophenotype: CD5 (≤75%) (n=111)						
ETP immunophenotype	3	(3%)	1	(14%)	0,23	
non ETP immunophenotype	101	(97%)	6	(86%)		
CD1-, CD4/CD8 DN, CD34/CD33/CD13+ (n=111)						
yes	12	(12%)	4	(57%)	0,008	0.0033
no	92	(88%)	3	(43%)		
Chromosomal rearrangements (n=117)						
TAL1/2/LYL1 (n=27)	27	(24%)	0	(0%)	0.2	
LMO1/2/3 (n=14)	14	(13%)	0	(11%)	0.6	
TLX3 (n=22)	22	(20%)	0	(0%)	0.35	
TLX1 (n=7)	7	(6%)	0	(0%)	1	
HOXA (n=10)	9	(8%)	1	(22%)	0.47	
MEF2C (n=6)	3	(2%)	3	(33%)	0.002	0.003
NKX2-1/NKX2-2 (n=7)	7	(6%)	0	(0%)	1	
Unknown (n=26)	23	(21%)	3	(33%)	0.18	
Unsupervised T-ALL clusters (n=116)						
TAL/LMO (n=53)	52	(48%)	1	(14%)		
Proliferative (n=19)	19	(17%)	0	(0%)		
Immature (n=15)	9	(8%)	6	(86%)	<0.001	0.0028
TLX (n=29)	29	(27%)	0	(0%)		
NOTCH1/FBXW7 status (n=112)						
wild-type (n=42)	39	(37%)	3	(43%)	1	
mutant (n=70)	66	(63%)	4	(57%)		
PTEN/AKT status (n=113)						
wild-type (n=95)	85	(80%)	7	(100%)	0.35	
mutant (n=18)	21	(20%)	0	(0%)		
PHF6 status (n=41)						
wild-type (n=32)	31	(78%)	1	(100%)	1	
mutant (n=9)	9	(22%)	0	(0%)		
WT1 status (n=115)						
wild-type (n=100)	93	(93%)	7	(100%)	0.59	
mutant (n=15)	15	(7%)	0	(0%)		

Unsupervised clusters are explained in the legend for Table 3. Significant *p*-values are indicated in bold. The *p*-values were calculated using the Fisher's exact test or the Pearson's Chi-square test (#) instead: * Mann-Whitney *U* test. ^The significance level of ABD frequencies within the indicated cytogenetic subtypes was compared to all other subtypes. ABD, Absence of bi-allelic TCR-gamma deletions; yr, year; WBC, white blood cell count; Bonferroni-Holm significance level for multiple testing correction is indicated.

Supplementary Table S6. Increased expression of hematopoietic progenitor population signature genes in the immature cluster gene signature.

significance levels for enriched signature gene selections in the Immature cluster signature (784 genes)

Threshold for gene selection	1.00E-09		1.00E-08		1.00E-07		1.00E-06		1.00E-05	
	Genes	<i>p</i> -value	Genes	<i>p</i> -value	Genes	<i>p</i> -value	Genes	<i>p</i> -value	Genes	<i>p</i> -value
Signatures from Novershtern <i>et al.</i>, 2011										
B-cell down-regulated	44	0.0015231	80	0.00079029	124	0.0039393	214	0.025091	317	0.082069
B-cell up-regulated	540	0.0019873	646	0.00053342	827	0.0012076	1059	0.0011589	1286	0.0003373
ERY down-regulated	801	0.12107	973	0.23755	1171	0.40063	1414	0.30715	1647	0.34433
ERY up-regulated	830	0.42728	914	0.51118	1007	0.58083	1144	0.45755	1227	0.55181
GMP down-regulated	6	0.030566	7	0.03557	10	0.050427	28	0.13492	58	0.036192
GMP up-regulated	325	1	400	1	484	1	598	0.40081	699	0.29357
HSC down-regulated	3	1	7	1	14	1	35	1	59	1
HSC/ early ERY down-regulated	188	0.62328	252	0.6259	360	0.44348	473	0.55774	586	0.41461
HSC/ early ERY up-regulated	1020	0.0065799	1163	0.0071626	1310	0.0077648	1509	0.011102	1687	0.027455
HSC up-regulated	355	0.0024999	452	0.0091381	560	0.0086623	710	0.031054	872	0.0055616
Late ERY down-regulated	1400	0.29717	1603	0.44659	1854	0.24862	2112	0.2002	2334	0.14741
Late ERY up-regulated	947	0.27527	1013	0.39682	1095	0.50064	1181	0.59086	1269	0.51653
NK down-regulated	19	1	33	0.15704	64	0.28216	137	0.15766	249	0.36856
NK up-regulated	41	1	52	1	73	1	105	1	133	0.49837
T-cell down-regulated	314	0.0058655	392	0.016251	510	0.016784	658	0.0071884	797	0.00088026
T-cell up-regulated	1071	0.050717	1236	0.055021	1423	0.11768	1669	0.089891	1868	0.1668